Journal of Biomolecular NMR, **18:** 153–164, 2000.
KLUWER/ESCOM

Redor in IS_1S_2 systems

Jörg Leppert, Bert Heise & Ramadurai Ramachandran*
Abteilung Molekulare Biophysik/NMR Spektroskopie, Institut für Molekulare Biotechnologie, D-07745 Jena, Germany

Received 23 March 2000; Accepted 7 August 2000

Key words: chemical shift tensors, MAS, REDOR, solid state NMR

Abstract

An approach to the determination of the 2-$^{13}C'$ chemical shift (CS) tensor orientation in pyrimidine bases via heteronuclear MAS NMR spectroscopy is presented. Considering a dipolar coupled spin 1/2 network of the type S_1-I-S_2 consisting of directly bonded heteronuclear spins, we have carried out numerical simulations to assess the sensitivity of I-S REDOR spinning sidebands to the Euler angles defining the orientation of the I-S_1 and I-S_2 dipolar vectors in the I spin CS tensor principal axes system. Our investigations clearly demonstrate the potential of I-S REDOR studies in IS_1S_2 systems for obtaining with high reliability and accuracy the I spin chemical shift tensor orientation in the molecular frame spanned by the two internuclear vectors I-S_1 and I-S_2. The significant contribution to the observed REDOR sideband intensities from anti-phase operator terms which are present at the start of the data acquisition is illustrated. The procedure for the recording and analysis of the I-S REDOR spectra in IS_1S_2 systems is presented and the measurement of the 2-$^{13}C'$ CS tensor orientation in a polycrystalline sample of [1,3-$^{15}N_2$, 2-^{13}C] uracil, which is one of the four bases in RNA, is experimentally demonstrated.

Introduction

RNAs are polynucleotides containing ribose sugars connected by 3′-5′ phosphodiester linkages. The pyrimidine (uracil and cytosine) and purine (adenine and guanine) bases are connected to the ribose sugar in the β-position of the anomeric carbon. RNAs play a critical role in a multitude of biological processes and exhibit a variety of secondary and tertiary structural features (Gesteland and Atkins, 1993) which are stabilized via hydrogen bonding. The ability of RNAs to adopt a range of folding topologies has been found to be responsible for its catalytic properties and its intimate role in gene expression and regulation.

The introduction of new molecular biological techniques for the production of ^{13}C and ^{15}N labelled RNAs has certainly advanced the application of multidimensional solution state NMR to structural investigations of RNAs (Varani et al., 1996; Wijmenga and van Buuren, 1998). The availability of labelled RNAs has permitted the development of a variety of novel schemes for sequential resonance assignments (Farmer et al., 1994; Simorre et al., 1995, 1996a, b; Sklenar et al., 1996, 1998; Sich et al., 1996; Ramachandran et al., 1996, 1997; Fiala et al., 1996; Dieckmann and Feigon, 1997; Dayie et al., 1998; Kolk et al., 1998; Wöhnert et al., 1999), a prerequisite for any NMR based structure determination. This has enabled the elucidation of NMR derived structures of RNAs of up to ∼40 nucleotides (Jucker and Pardi, 1995; Aboul-Ela et al., 1995; Jiang et al., 1996; Sich et al., 1997; Stoldt et al., 1999). Many of the hetero-atom based pulse schemes for sequential RNA resonance assignment involve pulse trains having large inter-pulse delays compared to the typical transverse relaxation times. It therefore appears that it may be difficult to substantially increase the molecular weight limit of RNAs that can be structurally investigated by solution state NMR methods (Varani et al., 1996; Wijmenga and van Buuren, 1998). The difficulties in dealing with large RNAs, unless overcome by the recent advances in NMR solution structure determina-

*To whom correspondence should be addressed. E-mail: raman@imb-jena.de

tion procedures (Mollova et al., 2000), may preclude one from obtaining a better understanding of several important issues such as the relationship between RNA folding and its biological function, relationship between sequence and global conformation. X-ray crystallography is an alternative approach for structural studies. Advances in crystallisation procedures have enabled the determination of several RNA structures in recent years (Varani et al., 1996; Holbrook and Kim, 1997; Frankel, 2000). However, the difficulties in obtaining RNA crystals diffracting to high resolution and to obtain the heavy metal derivatives hamper the routine usage of X-ray crystallography in the study of RNAs. In view of the fact that RNAs constitute an important class of biomolecules, it is imperative that one should also explore alternative possibilities to experimentally determine RNA structures by making use of the recent advances in the preparation of site selectively, base/strand/segment specifically and uniformly labelled RNAs (Batey et al., 1992; SantaLucia et al., 1995; Xu et al., 1996; Dieckmann and Feigon, 1997).

Solid state NMR (Schmidt-Rohr and Spiess, 1994) is one such approach which is yet to be exploited in structural studies of RNAs. High resolution solid state NMR spectra of spin $\frac{1}{2}$ nuclei from powder samples can be obtained under magic angle spinning (MAS) conditions. Although MAS attenuates dipolar interactions, in recent years a plethora of powerful dipolar recoupling techniques for inhibiting the spatial averaging of weak dipolar couplings have been introduced. This has opened up possibilities for the measurement of structurally relevant weak dipolar couplings and thereby long-range distances (Gullion and Schaefer, 1989; Bennett et al., 1994; Griffin, 1998). For the measurement of distances between homonuclear dipolar coupled spins such as ^{13}C, a variety of recoupling schemes (Bennett et al., 1994; Griffin, 1998) with varying degrees of performance characteristics have been developed and the potential of these dipolar recoupling schemes for distance measurements has been illustrated in a variety of systems. Indeed, employing the DRAWS sequence, ^{13}C-^{13}C distance measurements in several DNA dodecamers have been successfully carried out (Mehta et al., 1996; Gregory et al., 1997). A knowledge of the CS tensor orientation in the local molecular frame is often needed in the context of distance measurements via many of the homonuclear dipolar recoupling schemes mentioned above and could also be of value in other investigations such as cross-correlated relaxation studies in liquids (Yang et al., 1997).

As mentioned earlier, hydrogen bonding plays an important role in providing structural stability to RNAs and solid state NMR could be effectively used to characterize hydrogen bonding. In recent studies it has been pointed out that a measurement of the anisotropy of the chemical shift tensor, its magnitude and orientation rather than the isotropic chemical shift alone can provide a much better understanding of the electronic environment around a nucleus and how it is influenced by hydrogen bonding (Anderson-Altman et al., 1995; Facelli et al., 1995; Asakawa et al., 1998; Takeda et al., 1999). In RNA bases, the nitrogen nuclei and carbonyl carbons, through its directly bonded oxygen, play an active role in hydrogen bonding. Hence, a study of the ^{15}N and ^{13}C′ chemical shift tensors of the bases in RNAs is relevant and it is important to have the necessary experimental techniques for the characterisation of CS tensors.

Solid state NMR has been the natural method of choice for the characterization of chemical shift tensors. While single crystal based studies of chemical shift tensors (Takeda et al., 1999) are rare due to the difficulties in obtaining large single crystals, static NMR measurements on polycrystalline specimens are not attractive as the limited spectral resolution seen in such studies (Hartzell et al., 1987; Lorigan et al., 1999) precludes the simultaneous characterization of CSAs of multiple sites. While the magnitude of the CS tensor principal values can be conveniently obtained from conventional CPMAS spectra, one has to employ more advanced techniques for obtaining the CS tensor orientations. We have recently shown that heteronuclear MAS NMR techniques can be effectively employed to characterize the ^{15}N CS tensor in a ^{1}H-^{15}N-^{13}C dipolar network (Heise et al., 2000). As part of our ongoing efforts on the characterization of chemical shift tensors in nucleic acid bases and in multiply ^{15}N labelled systems with resolved isotropic ^{15}N chemical shifts, we have measured recently the chemical shift tensor orientation for the two ^{15}N sites in uracil (Leppert et al., 2000). In our approach we employ ^{15}N-^{13}C REDOR (Gullion and Schaefer, 1989) and ^{15}N-^{1}H DIPSHIFT (Munowitz and Griffin, 1982, 1983) experiments to obtain the Euler angles defining the orientation of the N-C and N-H dipolar vectors in the ^{15}N CS tensor principal axes system. In this work we extend our heteronuclear MAS NMR studies to the characterization of 2-^{13}C′ CS tensors of the pyrimidine bases. As two nitrogens are directly bonded to the pyrimidine 2-^{13}C′, we have considered a dipolar coupled spin network of the type $^{15}N_1$-^{13}C-$^{15}N_2$. We

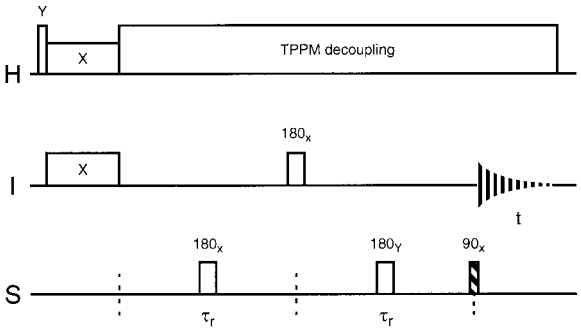

Figure 1. REDOR sequence with a 90° purging pulse at the start of the data acquisition and 180° dephasing pulses at the centre of the rotor periods.

have carried out numerical simulations to assess the sensitivity of ^{13}C-^{15}N REDOR spinning sidebands to the Euler angles defining the orientation of the ^{13}C-^{15}N$_1$ and ^{13}C-^{15}N$_2$ dipolar vectors in the ^{13}C CSA frame.

Our investigations clearly demonstrate that the REDOR spinning sidebands are extremely sensitive to the Euler angles. Hence, the orientation of the 2-^{13}C′ CS tensor can be measured with high accuracy and reliability via a ^{13}C-^{15}N REDOR experiment. The procedure for the recording and analysis of the REDOR spectra in systems of the type ^{15}N$_1$-^{13}C-^{15}N$_2$ is presented. The method has been experimentally demonstrated, as an example, by a measurement of the 2-^{13}C′ CS tensor orientation in a polycrystalline sample of [1,3-^{15}N$_2$,2-^{13}C] uracil.

Numerical procedures

We have employed a two rotor period REDOR sequence (Figure 1) in our investigations and we neglect scalar couplings and homonuclear dipolar interactions in our calculations. For a dipolar coupled spin $\frac{1}{2}$ network S$_1$-I-S$_2$, the MAS Hamiltonian in the rotating frame is given by (Olejniczak et al., 1984; Leppert et al., 1999a):

$$\begin{aligned} H(t) = \; & \Delta\omega I_Z - \omega_I[g_1\cos(\omega_r t + \phi_1) \\ & + g_2\cos(\omega_r t + \phi_2)]I_Z \\ & + \omega_{IS_1}[D_1\cos(\omega_r t - \alpha_{D1}) \\ & + G_1\cos(2\omega_r t - 2\alpha_{D1})]I_Z S_{1Z} \\ & + \omega_{IS_2}[D_2\cos(\omega_r t - \alpha_{D2}) \\ & + G_2\cos(2\omega_r t - 2\alpha_{D2})]I_Z S_{2Z} \end{aligned}$$

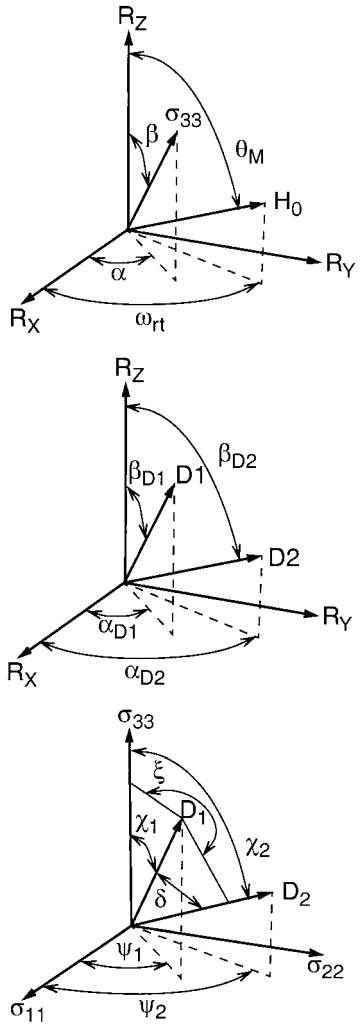

Figure 2. Orientation of the external magnetic field H$_0$, the Z principal axis σ_{33} of the CS tensor and the dipolar vectors (D$_1$, D$_2$) in the rotor frame (R$_X$, R$_Y$, R$_Z$) and the dipolar vectors in the CSA principal axes (σ_{11}, σ_{22}, σ_{33}) system.

where

$$\begin{aligned} \Delta\omega &= [\tfrac{1}{3}\omega_0(\sigma_{11}+\sigma_{22}+\sigma_{33}) + \omega_{off}], \\ \omega_I &= \omega_0[\sigma_{33} - \tfrac{1}{3}(\sigma_{11}+\sigma_{22}+\sigma_{33}], \\ g_1 &= \tfrac{1}{2}\sin(2\theta_m)\sin\beta[(\eta\cos 2\gamma + 3)^2\cos^2\beta \\ &\quad + \eta^2\sin^2 2\gamma]^{1/2}, \\ g_2 &= \tfrac{1}{2}\sin^2\theta_m[(\tfrac{3}{2}\sin^2\beta - \frac{\eta}{2}\cos 2\gamma(1+\cos^2\beta))^2 \\ &\quad + \eta^2\cos^2\beta\sin^2 2\gamma]^{1/2}, \\ \phi_1 &= \alpha + \varphi_1, \\ \phi_2 &= 2\alpha + \varphi_2, \\ D_{1,2} &= 2\sqrt{2}\cdot\sin\beta_{D_{1,2}}\cos\beta_{D_{1,2}} \end{aligned}$$

and

$$G_{1,2} = \sin^2\beta_{D_{1,2}}.$$

In the above equation, φ_1, φ_2 and η are defined as

$$\tan\varphi_1 = \frac{\eta \sin 2\gamma}{\cos\beta[\eta\cos 2\gamma + 3]},$$

$$\tan\varphi_2 = \frac{-\eta\cos\beta\sin 2\gamma}{\frac{3}{2}\sin^2\beta - \frac{\eta}{2}\cos 2\gamma(1+\cos^2\beta)}$$

and

$$\eta = \frac{\sigma_{22} - \sigma_{11}}{\sigma_{33} - \frac{1}{3}Tr(\sigma)}.$$

(α,β,γ) are the Euler angles defining the orientation of the CS tensor in the rotor frame (Figure 2), (σ_{11}, σ_{22}, σ_{33}) are the principal values of the CS tensor, ω_0 is the Larmor frequency, θ_m is the magic angle (Figure 2) and ω_{off} is the resonance offset. $\alpha_{D1,2}$ is the azimuthal angle of the dipolar vector in the rotor frame (Figure 2) and $\omega_{IS_{1,2}}$ are the dipolar coupling strengths. The polar and azimuthal angles ($\beta_{D1,2}$, $\alpha_{D1,2}$) are related to the angles (α, β, γ) and the polar and azimuthal angles ($\chi_{1,2}$, $\Psi_{1,2}$) of the dipolar vectors in the CSA frame (Figure 2) as

$$\cos\beta_D = \cos\chi\cos\beta - \sin\chi\sin\beta\cos(\gamma+\Psi),$$

$$\alpha_D = \alpha + \cos^{-1}\left(\frac{\cos\chi - \cos\beta\cdot\cos\beta_D}{\sin\beta\cdot\sin\beta_D}\right).$$

Assuming ideal experimental conditions and delta pulses we have studied the evolution of the spin system under the RF pulse sequence given in Figure 1 via standard density matrix calculations. lt is seen from these calculations that, following cross polarization and starting from a density matrix corresponding to the I_x operator, the system evolves under the sequence such that at the beginning of the data acquisition the density operator has contributions from four different single quantum product operator terms of the type I_X, $I_Y S_{1Z}$, $I_Y S_{2Z}$ and $I_X S_{1Z} S_{2Z}$.

In some situations, the strength of the heteronuclear dipolar coupling may not be negligible in comparison to the spinning speed employed. Under these circumstances, the anti-phase operator terms can evolve under the incompletely averaged heteronuclear dipolar interactions to refocus to an in-phase I_X term and thereby contribute to the observed REDOR signal (Leppert et al., 1999b). In the case of the three spin system studied here we find that the observed I-S REDOR signal for a single crystallite is given by:

$$\begin{aligned}\langle I^+(\chi_1,\Psi_1,\chi_2,\Psi_2)\rangle = {} & [\cos A_1\cos B_1\cos A_2\cos B_2 \\ & + \sin A_1\sin B_1\cos A_2\cos B_2 \\ & + \cos A_1\cos B_1\sin A_2\sin B_2 \\ & + \sin A_1\sin B_1\sin A_2\sin B_2] \\ & \exp(iC)\end{aligned}$$

where

$$A_{1,2} = 4D_{1,2}\left(\frac{\omega_{IS_{1,2}}}{\omega_r}\right)\sin\alpha_{D_{1,2}},$$

$$\begin{aligned}B_{1,2} = {} & \frac{\omega_{IS_{1,2}}}{4\omega_r}\cdot[2D_{1,2}\sin(\omega_r t - \alpha_{D_{1,2}}) \\ & + G_{1,2}\sin 2(\omega_r t - \alpha_{D_{1,2}}) \\ & + 2D_{1,2}\sin\alpha_{D_{1,2}} \\ & + G_{1,2}\sin 2\alpha_{D_{1,2}}]\end{aligned}$$

and

$$\begin{aligned}C = {} & \frac{\omega_I}{2\omega_r}\cdot[(2g_1\sin\phi_1 + g_2\sin\phi_2) \\ & - (2g_1\sin(\omega_r t + \phi_1) \\ & + g_2\sin(2\omega_r t + \phi_2))].\end{aligned}$$

A weighted averaging of the response over all possible crystallite orientations gives the final signal observed. The four terms in the expression for $\langle I^+\rangle$ arise respectively from the single quantum operator terms mentioned above. Under slow spinning conditions, under which our REDOR experiments were typically carried out, the contributions from the anti-phase operator terms to the observed signal intensity are found to be significant. lt should be noted that although these terms do not contribute to the net intensity of the observed signal, the presence of these terms leads to different REDOR spinning sideband intensity patterns compared to those seen in the absence of these terms. The contributions from the anti-phase operator terms can be eliminated either by decoupling the S-spin during the data acquisition or, in a simpler way, by the application of a 90 degree purging pulse on the dephasing channel at the start of the data acquisition (Leppert et al., 1999b). If the I-S REDOR experiment is carried out without the application of a purging pulse, then the REDOR sideband intensities have to be analyzed by taking into account all the four terms in $\langle I^+\rangle$.

The spectral simulations and the iterative fitting of the experimental spectra were carried out using the software 'SPINME' which is being developed in-house (Leppert et al., unpublished; Heise et al., 2000). Starting from known values of the CS tensor principal values and dipolar coupling strengths, the powder averaged REDOR signal is calculated with some initial values of the Euler angles ($\chi_{1,2}$, $\Psi_{1,2}$). The resultant time domain signal is subjected to a discrete Fourier transform step to obtain the REDOR spectral sideband intensities.

Employing the Nelder-Mead Simplex local-optimization algorithm (Press et al., 1986), the starting initial

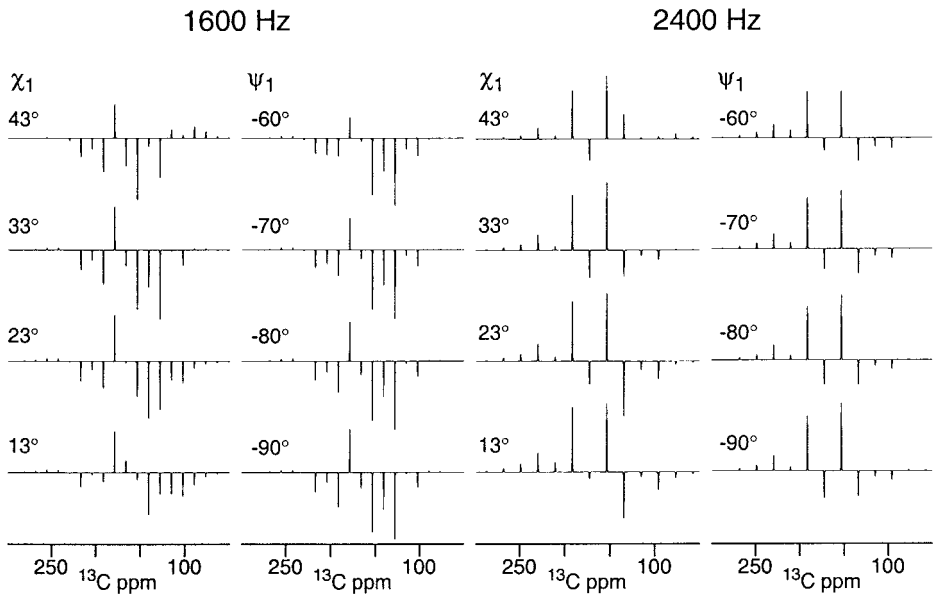

Figure 3. Simulated plots of purged I-S REDOR spectra in a IS_1S_2 system as a function of the angles χ_1 and Ψ_1 as indicated and at spinning speeds of 1600 and 2400 Hz. The plots were obtained employing a I-S dipolar coupling of 1110 Hz and CS tensor principal values of (σ_{11}, σ_{22}, σ_{33}) = (94.5 ppm, 135.2 ppm, 230.2 ppm). In the simulated plots where χ_1 is varied, (Ψ_1, χ_2, Ψ_2) were set to ($-90°$, 147°, $-90°$) and in the plots where Ψ_1 is varied, (χ_1, χ_2, Ψ_2) were set to (33°, 147°,$-90°$).

values of the Euler angles are optimized through an iterative process until the calculated sideband amplitudes are in satisfactory agreement with the experimental data. In some situations, the angle δ (Figure 2) between the two dipolar vectors is known, for example from crystallographic studies. To minimize the computational time, the optimization problem can then be simplified to a searching of a parameter space of only three variables (χ_1, Ψ_1, ξ) (Figure 2) via the following transformations:

$$\cos\chi_2 = \cos\chi_1 \cdot \cos\delta + \sin\chi_1 \cdot \sin\delta \cdot \cos\xi$$

$$\cos(\Psi_2 - \Psi_1) = (\cos\delta - \cos\chi_1 \cdot \cos\chi_2)/(\sin\chi_1 \cdot \sin\chi_2)$$

Experimental

All experiments were performed at room temperature on a 500 MHz wide bore Varian^{UNITY} *INOVA* solid state NMR spectrometer equipped with a 5 mm XC5 DOTY supersonic triple resonance probe. Cross-polarization under Hartmann–Hahn matching conditions was applied and typical ^{1}H, ^{15}N and ^{13}C 90 degree pulse widths of 3.5, 6.5 and 4.4 μs were used,

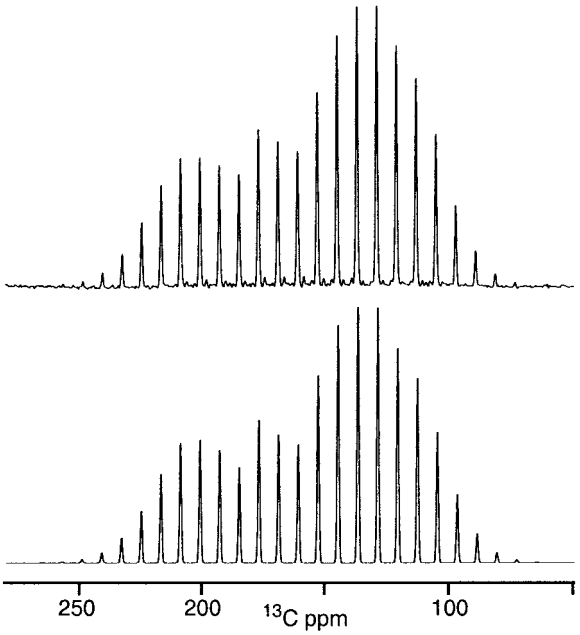

Figure 4. Experimental (top) ^{13}C CPMAS spectra of 2-^{13}C′ labelled uracil at a spinning speed of 1000 Hz. The simulated (bottom) plot was obtained employing the estimated CSA parameters (σ_{11}, σ_{22}, σ_{33}) of (94.5 ppm, 135.2 ppm, 230.2 ppm).

respectively. All spectra were collected under high power ^{1}H TPPM decoupling (Bennett et al., 1995) and were referenced indirectly relative to DSS (Wishart et al., 1995). Other relevant experimental parameters are given in the figure captions. Labelled 2-^{13}C and 2-^{13}C, $^{15}N_2$ uracil samples were prepared as reported in the literature (Anderson-Altman et al., 1995) from labelled urea obtained from Isotec, Inc. Of each sample, 26 mg was packed into a small, cylindrical 70 μl Kel-F insert and kept at the centre of the rotor to provide good H_1 homogeneity throughout the sample volume.

Results and discussion

To assess the sensitivity of the I-S REDOR spectra in IS_1S_2 systems to the Euler angles defining the orientation of the dipolar vectors in the CS tensor principal axes system, 1D simulated REDOR spectra were obtained as a function of the angles. Figure 3 shows the spectra at two representative MAS spinning speeds. For generating these plots, the $^{13}C'$ CS tensor values and C-N dipolar couplings seen in uracil were employed. From crystal structure data (Stewart and Jensen, 1967; Clowney et al., 1996) and from our recent ^{15}N-^{13}C REDOR studies on uracil (Leppert et al., 2000), it is seen that one can safely assume the same value for both dipolar couplings. The simulated REDOR plots shown in Figure 3 have been obtained employing a value of 1110 Hz for the I-S dipolar couplings. In the simulated plots where χ_1 is varied, (Ψ_1, χ_2, Ψ_2) were set to (-90, 147, -90) and in the plots where Ψ_1 is varied, (χ_1, χ_2, Ψ_2) were set to (33, 147, -90). The angles employed in our simulations correspond to the values obtained for uracil (see below). With a typical N-C dipolar coupling of ∼1 kHz, it is seen that with the two rotor period REDOR sequence shown in Figure 1, the sensitivity of the purged REDOR spectra to the Euler angles is excellent at spinning speeds where the REDOR dephasing is high, e.g., 1600 Hz. A similar sensitivity to the angles is also seen for the unpurged data (spectra not shown). At higher spinning speeds, where the REDOR reduction is not significant, the sensitivity to the Euler angles is not pronounced. However, it may be possible to collect REDOR spectra at higher spinning speeds and with good sensitivity to the angles by employing more than two rotor periods of dipolar recoupling (Heise et al., 2000). The sensitivity of the REDOR spectra to the angles is also seen from 2D RMSD plots, discussed later in the text.

For the iterative analysis of experimental REDOR spectra, the $^{13}C'$ CS tensor principal values are first obtained from $^{13}C'$ CPMAS spectra of [2-$^{13}C'$] uracil recorded at different spinning speeds. The σ_{11}, σ_{22} and σ_{33} values were found to be (94.5, 135.2, 230.2) ppm. Figure 4 shows as an example a $^{13}C'$ CPMAS experimental spectrum at a spinning speed of 1000 Hz and the corresponding simulated spectrum obtained with the estimated CS tensor principal values.

Experimental and corresponding simulated unpurged and purged I-S REDOR plots at different spinning speeds are shown in Figures 5 and 6, respectively. The optimized angles (χ_1, Ψ_1, χ_2, Ψ_2) obtained from an iterative analysis of the REDOR data collected at lower spinning speeds (1600, 2000 Hz) were found to be (33, -90, 147, -90) with the σ_{22} and σ_{33} in the molecular plane. These estimated angles and the CS tensor principal values given above were used in all simulations. The spectra shown in Figures 5 and 6 also clearly confirm our earlier observation (Leppert et al., 1999b) that the contribution from the anti-phase operator terms cannot be neglected in the analysis of REDOR spectra recorded at low spinning speeds and when one is dealing with significant heteronuclear dipolar couplings. As seen from Figures 5 and 6, appreciable differences in the purged and unpurged REDOR sideband intensities can be observed even at a spinning speed of 3600 Hz.

Although we have estimated earlier the N-C dipolar coupling in uracil to be ∼1020 Hz via N-C REDOR experiments (Leppert et al., 2000), employing an undiluted sample of [2-^{13}C, $^{15}N_2$] uracil, the best fitting simulated C-N REDOR data could only be obtained using a dipolar coupling of 1110 Hz (such differences can possibly arise due to intermolecular interactions which could be minimized by a dilution of the labelled with unlabelled uracil). The value of 1110 Hz for the dipolar coupling was obtained by varying it in the range of ∼1000–1200 Hz and for each value employed, the REDOR spectra were iteratively analysed to obtain the Euler angles (χ_1, Ψ_1, χ_2, Ψ_2). The dipolar coupling strength was fixed at the value at which a good fit between simulated and experimental data over all spinning speeds was obtained. lt is seen (Figures 5 and 6) that with a value of 1110 Hz for the dipolar coupling, the experimental REDOR sideband intensities can be fitted well with the estimated Euler angles of (33, -90, 147, -90). The moderate sensitivity of the REDOR spectra to small variations in the dipolar coupling strength is shown in Figure 7. These simulated purged REDOR plots were obtained at a spinning

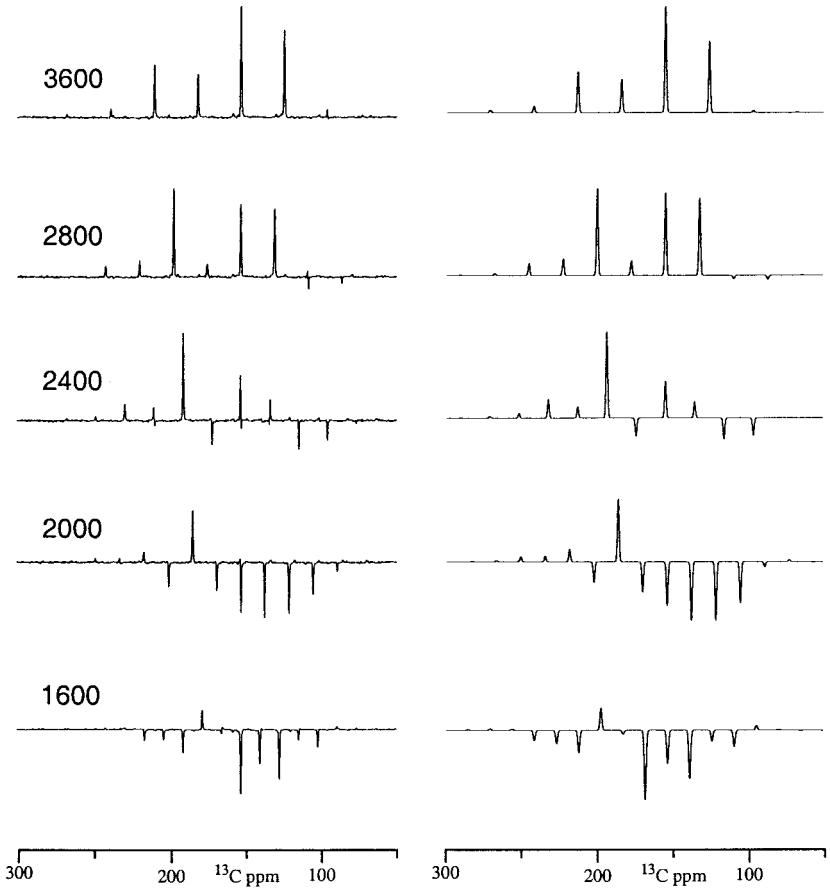

Figure 5. Experimental unpurged ^{13}C-^{15}N REDOR spectra (left) of 2-^{13}C′, $^{15}N_2$ uracil and the corresponding simulated spectra (right) at the spinning speeds indicated (in Hz). The spectra were recorded with a recycle time of 64 s and 8, 16, 32, 48 and 128 scans at the spinning speeds of 3600, 2800, 2400, 2000 and 1600 Hz, respectively. The simulated plots were obtained employing the CSA parameters as in Figure 4 and dipolar couplings of 1110 Hz. The Euler angles (χ_1, Ψ_1, χ_2, Ψ_2) were set to (33, −90, 147, −90).

speed of 1600 Hz by varying both dipolar couplings simultaneously (A) and by varying only the I-S_2 dipolar couplings with I-S_1 fixed at 1110 Hz (B).

As seen from Figure 7 a value of ∼1110 Hz for both dipolar coupling strengths leads to a simulated purged REDOR spectrum that matches well with the experimental data given in Figure 6.

To get an idea about the error margin in the estimated Euler angles we have carried out an RMSD calculation based on established procedures (Hong et al., 1998; Leppert et al., 2000). In this we first calculate a simulated spectrum for a given set of angles. Then we calculate the RMSD between this spectrum and the spectrum generated for different values of the Euler angles (in our case we have obtained the RMSD plots by fixing two angles and by varying the other two angles). The 2D plots thus generated are shown in Figure 8. lt is seen that the angles can be estimated, for the same magnitude of the rms noise, with higher accuracy at low spinning speeds. With small rms noise the uncertainty in the estimated angles is essentially the same in the unpurged and purged REDOR spectra.

The orientations of the dipolar vectors in uracil are, as expected, essentially the same as those seen in thymidine for which the relevant angles have been obtained by Gregory et al. (1997) via static powder pattern analysis (the CSA values seen in uracil are slightly different from those of thymidine and the latter values did not fit the data given here). In fact, we have used the Euler angles seen in thymidine as the starting point in our iterative analysis to obtain the relevant angles for uracil. lt is worth pointing out that in the absence of a good starting point one may have to

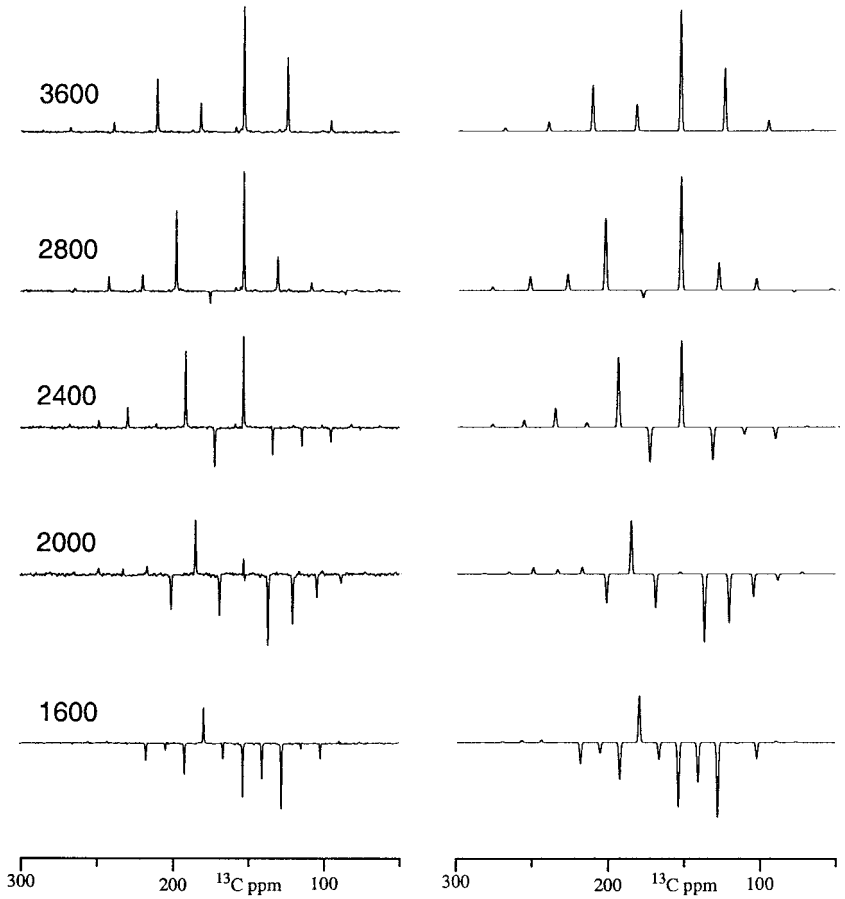

Figure 6. Experimental purged ^{13}C-^{15}N REDOR spectra (left) of 2-^{13}C′, $^{15}N_2$ uracil and the corresponding simulated spectra (right) at the spinning speeds indicated (in Hz). The experimental conditions were the same as in Figure 5. The simulated plots were obtained employing the CSA parameters, dipolar couplings and the Euler angles as in Figure 5.

take recourse to global optimization procedures such as simulated annealing (Press et al., 1986).

The CS tensor orientation of the 2-^{13}C′ carbon in uracil can also be obtained from two separate REDOR experiments carried out on two different samples, each having only one of the ^{15}N labelled sites. The results presented here suggest that with a single REDOR experiment and a single sample, it is possible to get the same information, provided a suitably labelled system is available (in the case of uracil, it is even easier to synthesize the [1,3-^{15}N,2-^{13}C] uracil than the [1-^{15}N,2-^{13}C] and [3-^{15}N-2-^{13}C] labelled uracil molecules).

Unlike static solid state NMR based techniques, the REDOR method can be conveniently employed to characterize multiple sites simultaneously. A MAS based approach is also advantageous in the context of fast iterative data analysis. Spectral sideband intensities at integral multiples of the spinning speed can be easily obtained from the time domain data, calculated for only one rotor period, by discrete Fourier analysis. Such fast calculations are very advantageous in any iterative analysis based parameter estimation (de Groot et al., 1991). As seen from Figure 9, the dipolar coupled ^{13}C static powder spectra appear to be much less sensitive to the Euler angles in comparison with the REDOR data (Figure 3). Hence, a reliable extraction of orientational information from experimental static spectra (Figure 9) may sometimes become difficult. Additionally, the ability to collect data at different spinning speeds improves the possibilities to obtain reliable parameter estimates via the REDOR approach. In situations where too many lines lead to spectral overlaps in one-dimensional data one can take recourse to 2D experiments for obtaining

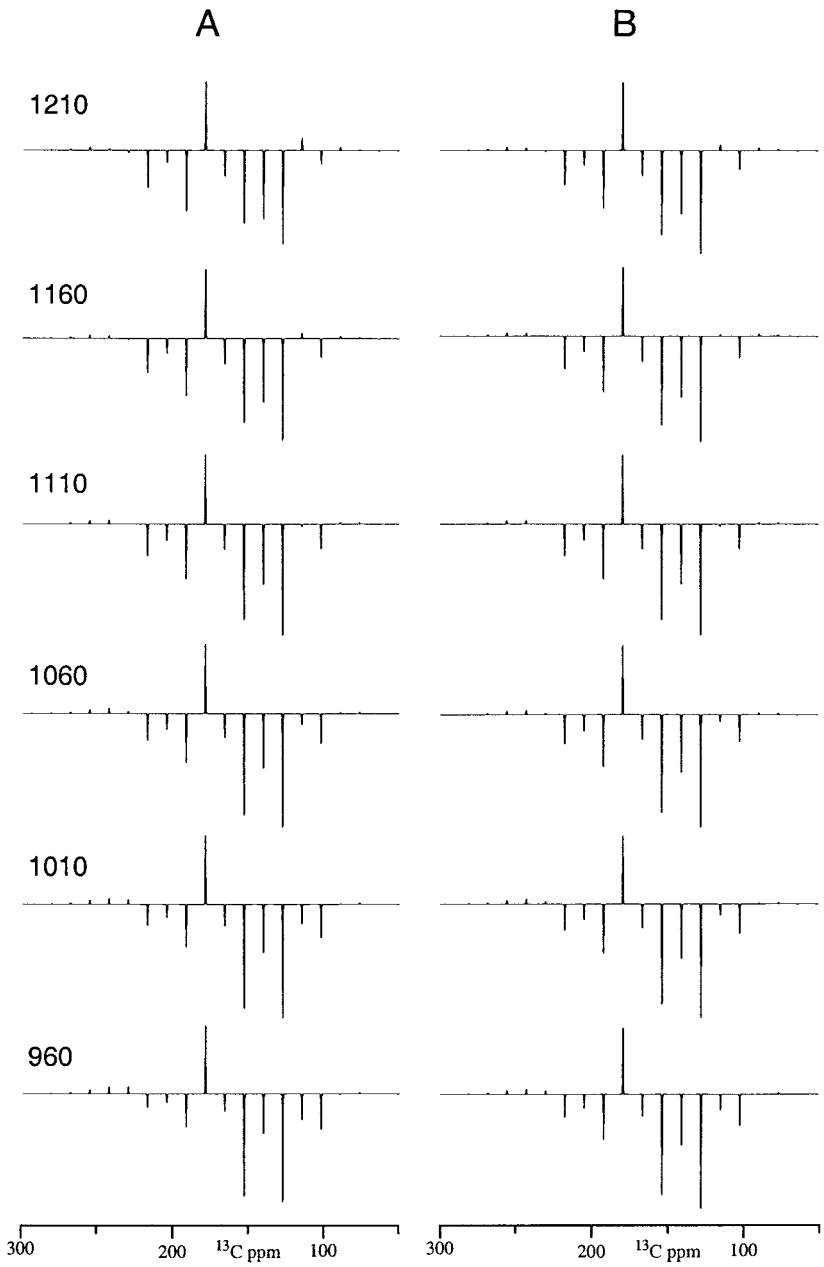

Figure 7. Simulated purged I-S REDOR plots in a IS_1S_2 system as a function of the dipolar coupling strength. These plots at 1600 Hz were obtained employing Euler angles and CS tensor values as in Figure 5. In A, both dipolar couplings I-S_1 and I-S_2 were varied as indicated. In B, the I-S_1 dipolar coupling was fixed at 1110 Hz and the I-S_2 dipolar coupling was varied as in A.

isotropic chemical shift resolved anisotropic data (Aue et al., 1981; Schmidt-Rohr, 1994).

Multispin systems have been dealt with earlier in the context of distance measurements via REDOR (Goetz and Schaefer, 1997; Nishimura et al., 1999; Bertmer and Eckert, 1999). The present work explores, for the first time, the possibilities for obtaining CS tensor orientation in the molecular frame from REDOR studies on systems containing multiple heteronuclear dipolar couplings. Although in this work we have employed selectively labelled uracil, the I-S REDOR experiment can possibly be applied to get orientational information from systems that are even multiply labelled with ^{13}C and ^{15}N. Since $^{13}C'$ CSA is

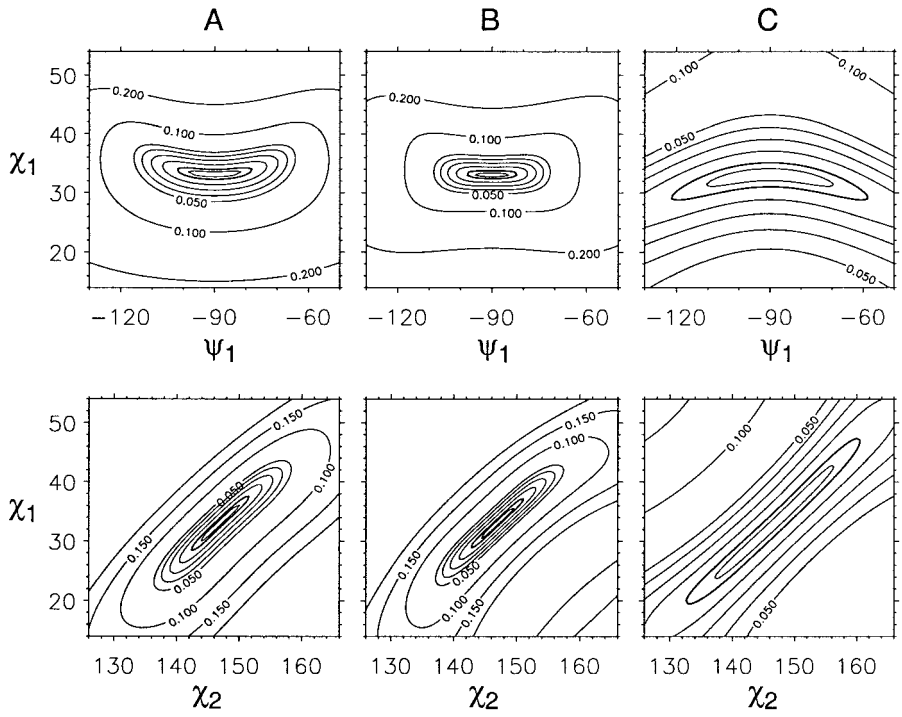

Figure 8. Plots of the RMSD between the simulated (A, 1600 Hz, unpurged; B, 1600 Hz, purged; C, 3600 Hz, purged) REDOR spectrum obtained employing Euler angles (χ_1, Ψ_1, χ_2, Ψ_2) of (33, −90, 147, −90) and the simulated spectra generated for (top) various values of (χ_1, Ψ_1) keeping (χ_2, Ψ_2) fixed at (147, −90) and (bottom) various values of (χ_1, χ_2) keeping (Ψ_1,Ψ_2) fixed at (−90, −90). The same CSA values and dipolar couplings as in Figure 5 were employed. The area enclosed by the darker contour line, which corresponds to the estimated experimental rms noise, provides a measure of the uncertainty in (χ_1, χ_2) and in (χ_1, Ψ_1).

relatively large, one can afford to carry out these experiments at moderate spinning speeds to minimise the effects of homonuclear ^{13}C-^{13}C dipolar couplings and yet retain a sufficient number of spinning sidebands for reliably extracting the orientational information. For example, if one has a fully ^{13}C and ^{15}N labelled uracil, the C2 carbon will experience dipolar coupling interactions with the C4, C5 and C6 carbons. These additional couplings to indirectly connected carbons can get sufficiently attenuated under MAS and the resultant data can possibly still be analysed to obtain orientational information. If such an approach fails, one can take recourse to multiple pulse homonuclear decoupling to further attenuate the residual ^{13}C-^{13}C homonuclear dipolar couplings (Schaefer, 1999). lt is also worth pointing out that in an I-S REDOR experiment, as we have done here, the only heteronuclear dipolar coupling interactions of relevance are I-S_1 and I-S_2. If the S spins experience additional couplings with some other I spins, such interactions would not affect the outcome of the I-S REDOR experiment.

The ability to characterise the CS tensor magnitude and orientation in RNAs would facilitate the creation of a database so that it may become possible to relate the measured values of the CS tensor parameters in a given system to the type of base pairing / hydrogen bonding. Depending upon the type of base pairing either the 2-$^{13}C'$ or the 4-$^{13}C'$ (through the attached oxygen) of the pyrimidine bases may be involved in hydrogen bonding and the CS tensor orientation of the latter has to be characterized via a different procedure that will be reported elsewhere. lt is also worth pointing out that the 2-$^{13}C'$ site in uracil crystals is not involved in intermolecular hydrogen bonding, as seen from X-ray studies (Parry, 1954; Stewart and Jensen, 1967), and hence the 2-$^{13}C'$ CS tensor orientation of uracil may be a representative of such an electronic environment.

The sensitivity of the I-S REDOR in IS_1S_2 systems to the Euler angles (χ_1, Ψ_1, χ_2, Ψ_2) suggests that this approach can also be effectively employed to characterize ^{15}N CS tensors in uniformly labelled medium sized peptides. Since the ^{15}N spins of the backbone are coupled directly to two carbons, it appears possible to obtain the CS tensor orientation of the ^{15}N nuclei via a single N-C REDOR experiment. As the

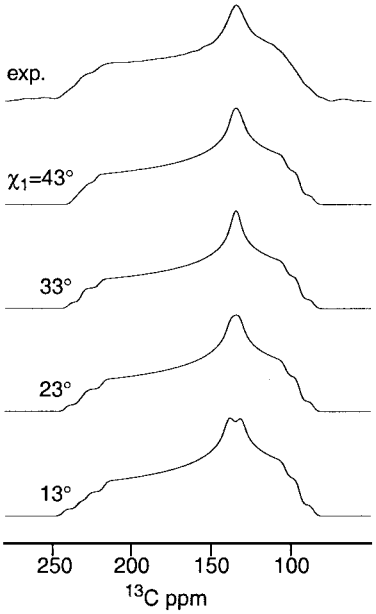

Figure 9. Experimental (top) static ^{13}C spectra of 2-$^{13}C'$ labelled uracil collected employing a spin echo sequence with 32 scans. The simulated spectra below were generated employing the same CS tensor and dipolar coupling values as in Figure 5. The angles (Ψ_1, χ_2, Ψ_2) were fixed at ($-90°$, 147°, $-90°$) and χ_1 was varied as indicated.

one bond ^{15}N-^{13}C dipolar coupling itself is only of the order of $\sim$1 kHz, long range ^{15}N-^{13}C dipolar interactions are not expected to substantially affect ^{15}N-^{13}C REDOR spectral data obtained with a small number of dipolar recoupling periods. If needed, the ^{15}N-^{13}C REDOR experiments in multiply ^{13}C labelled systems can also be carried out under ^{13}C-^{13}C homonuclear decoupling. The N-C REDOR approach can also be effective in situations where it is needed to obtain the ^{15}N CS tensor orientation for sites with no attached protons but with two attached carbons, as in the nucleic acid bases. Although the potential of REDOR studies on IS_1S_2 systems has been demonstrated here only on a simple system, the technique can be effectively employed, line width and signal to noise ratio permitting, on larger systems as well.

References

Aboul-Ela, E., Karn, J. and Varani, G. (1995) *J. Mol. Biol.*, **253**, 313–332.

Anderson-Altman, K.L., Phung, C., Mavromoustakos, G.S., Zheng, Z., Facelli, J.C., Poulter, C.D. and Grant, D.M. (1995) *J. Phys. Chem.*, **99**, 10454–10458.

Asakawa, N., Kameda, T., Kuroki, S., Kurosu, H., Ando, S., Ando, S. and Shoji, A. (1998) *Annu. Rep. NMR Spectrosc.*, **35**, 55–137.

Aue, W.P., Ruben, D.J. and Griffin, R.G. (1981) *J. Magn. Reson.*, **91**, 472–477.

Batey, R.T., Inada, M., Kujawinski, E., Puglisi, J.D. and Williamson, J.R. (1992) *Nucleic Acids Res.*, **17**, 4515–4525.

Bennett, A.E., Griffin, R.G. and Vega, S. (1994) *NMR Basic Principles and Progress*, Springer-Verlag, Berlin, **33**, 1–77.

Bennett, A.E., Rienstra, C.M., Auger, M., Lakshmi, K.V. and Griffin, R.G. (1995) *J. Chem. Phys.*, **103**, 6951–6958.

Bertmer, M. and Eckert, H. (1999) *Solid State Nucl. Magn. Reson.*, **15**, 139–152.

Clowney, L., Jain, S.C., Srinivasan, A.R., Westbrook, J., Olson, W.K. and Berman, H.M. (1996) *J. Am. Chem. Soc.*, **118**, 509–518.

Dayie, K.T., Tolbert, T.J. and Williamson, J.R. (1998) *J. Magn. Reson.*, **130**, 97–101.

Dieckmann, T. and Feigon, J. (1997) *J. Biomol. NMR*, **9**, 259–272.

Facelli, J.C., Gu, Z. and McDermott, A. (1995) *Mol. Phys.*, **86**, 865–872.

Farmer II, B.T., Müller, L., Nikonowicz, E.P. and Pardi, A. (1994) *J. Biomol. NMR*, **4**, 129–133.

Fiala, R., Jiang, E. and Patel, D.J. (1996) *J. Am. Chem. Soc.*, **118**, 689–690.

Frankel, A.D. (2000) *Curr. Opin. Struct. Biol.*, **10**, 332–340.

Gesteland, R.E and Atkins, J.E (Eds.) (1993) *The RNA World*, Cold Spring Harbor Laboratory Press, Cold Spring Harbor, NY.

Goetz, J.M. and Schaefer, J. (1997) *J. Magn. Reson.*, **127**, 147–154.

Gregory, D.M., Mehta, M.A., Shiels, J.C. and Drobny, G.P. (1997) *J. Chem. Phys.*, **107**, 1–42.

Griffin, R.G. (1998) *Nat. Struct. Biol.*, **5**, 508–512.

de Groot, H.J.M., Smith, S.O., Kolbert, A.C., Courtin, J.M.L., Winkel, C., Lugtenburg, J., Herzfeld, J. and Griffin, R.G. (1991) *J. Magn. Reson.*, **91**, 30–38.

Gullion, T. and Schaefer, J. (1989) *Adv. Magn. Reson.*, **13**, 57–83.

Hartzell, C.J., Pratum, T.K. and Drobny, G. (1987) *J. Chem. Phys.*, **87**, 4324–4331.

Heise, B., Leppert, J. and Ramachandran, R. (2000) *Solid State Nucl. Magn. Reson.*, **16**, 177–187.

Holbrook, S.R. and Kim, S.-H. (1997) *Biopolymers*, **44**, 3–21.

Hong, M., Gross, J.D., Hu, W. and Griffin, R.G. (1998) *J. Magn. Reson.*, **135**, 169–177.

Jiang, F., Kumar, R.A., Jones, R.A. and Patel, D.J. (1996) *Nature*, **382**, 183–186.

Jucker, F.M. and Pardi, A. (1995) *Biochemistry*, **34**, 14416–14427.

Kolk, M.H., Wijmenga, S.S., Heus, H.A. and Hilbers, C.W. (1998) *J. Biomol. NMR*, **12**, 423–433.

Leppert, J., Heise, B. and Ramachandran, R. (2000) *J. Magn. Reson.*, **145**, 307–314.

Leppert, J., Heise, B. and Ramachandran, R. (1999a) *J. Magn. Reson.*, **139**, 382–388.

Leppert, J., Heise, B. and Ramachandran, R. (1999b) *J. Magn. Reson.*, communicated.

Lorigan, G.A., McNamara, R., Jones, R.A. and Opella, S.J. (1999) *J. Magn. Reson.*, **140**, 315–319.

Mehta, M.A., Gregory, D.M., Kiihne, S., Mitchell, D.J., Hatcher, M.E., Shiels, J.C. and Drobny, G.P. (1996) *Solid State Nucl. Magn. Reson.*, **7**, 211–228.

Mollova, E.T. and Pardi, A. (2000) *Curr. Opin. Struct. Biol.*, **10**, 298–302.

Munowitz, M. and Griffin, R.G. (1982) *J. Chem. Phys.*, **76**, 2848–2858.

Munowitz, M. and Griffin, R.G. (1983) *J. Chem. Phys.*, **78**, 613–617.

Nishimura, K., Naito, A., Tuzi, S. and Salto, H. (1999) *J. Phys. Chem.*, **103**, 8398–8404.

Olejniczak, E.T., Vega, S. and Griffin, R.G. (1984) *J. Chem. Phys.*, **81**, 4804–4817.
Parry, G.S. (1954) *Acta Crystallogr.*, **7**, 313–320.
Press, W.H., Flannery, B.P., Teukolsky, S.A. and Vetterling, W.T. (1986) *Numerical Recipies: The Art of Scientific Computing*, Cambridge University Press, Cambridge.
Ramachandran, R., Sich, C., Grüne, M., Soskic, V. and Brown, L.R. (1996) *J. Biomol. NMR*, **7**, 251–255.
Ramachandran, R., Sich, C., Ohlenschläger, O. and Brown, L.R. (1997) *J. Magn. Reson.*, **124**, 210–213.
SantaLucia Jr., J., Shen, L.X., Zhuoping, C., Lewis, H. and Tinoco Jr., I. (1995) *Nucleic Acids Res.*, **23**, 4913–4921.
Schaefer, J. (1999) *J. Magn. Reson.*, **137**, 272–275.
Schmidt-Rohr, K. and Spiess, H.W. (1994) *Multidimensional Solid State NMR and Polymer*, Academic Press, London.
Sich, C., Flemming, J., Ramachandran, R. and Brown, L.R. (1996) *J. Magn. Reson.*, **B112**, 275–281.
Sich, C., Ohlenschläger, O., Ramachandran, R., Görlach, M. and Brown, L.R. (1997) Biochemistry, **36**, 13989–14002.
Simorre, J.-P., Zimmermann, G.R., Pardi, A., Farmer II, B.T. and Müller, L. (1995a) *J. Biomol. NMR*, **6**, 427–432.
Simorre, J.-P., Zimmermann, G.R., Müller, L. and Pardi, A. (1996a) *J. Am. Chem. Soc.*, **118**, 5316–5317.
Simorre, J.-P., Zimmermann, G.R., Müller, L. and Pardi, A. (1996b) *J. Biomol. NMR*, **27**, 153–156.
Sklenar, V., Dieckmann, T., Butcher, S.E. and Feigon, J. (1996) *J. Biomol. NMR*, **7**, 83–87.
Sklenar, V., Dieckmann, T., Butcher, S.E. and Feigon, J. (1998) *J. Magn. Reson.*, **130**, 119–124.
Stewart, R.E and Jensen, L.H. (1967) *Acta Crystallogr.*, **23**, 1102–1105.
Stoldt, M., Wöhnert, J., Ohlenschläger, O., Görlach, M. and Brown, L.R. (1999) *EMBO J.*, **18**, 6508–6521.
Takeda, N., Kuroki, S., Kurosu, H. and Ando, I. (1999) *Biopolymers*, **50**, 61–69.
Varani, G., Aboul-Ela, F. and Allain, F.H. (1996) *Progr. Nucl. Magn. Reson. Spectrosc.*, **29**, 51–127.
Wijmenga, S.S. and van Buuren, B.N.M. (1998) *Prog. Nucl. Magn. Reson. Spectrosc.*, **32**, 287–387.
Wöhnert, J., Ramachandran, R., Görlach, M. and Brown, L.R. (1999) *J. Magn. Reson.*, **139**, 430–433.
Wishart, D.S., Bigam, C.G., Yao, J., Abilgaard, E., Dyson, H.J., Oldfield, E., Markley, J.L. and Sykes, B.D. (1995) *J. Biomol. NMR*, **6**, 135–140.
Xu, J., Lapham, J. and Crothers, D.M. (1996) *Proc. Natl. Acad. Sci. USA*, **93**, 44–48.
Yang, D., Konrat, R. and Kay, L.E. (1997) *J. Am. Chem. Soc.*, **199**, 11938–11940.